(Schiff-base)Cu^{II} Complexes with Phenolate-Oxygen/Chloro or -Oxygen/Azido Mixed Bridges − Syntheses, Crystal Structures and Magnetic Properties

Yun-Bo Jiang,[a] **Hui-Zhong Kou,***[a] **Ru-Ji Wang,**[a] **and Ai-Li Cui**[a]

Keywords: Chloro bridges / Azido bridges / Magnetic properties / Cu^{II} ions / Crystal structures

Four new Cu^{II} complexes of formulae $[Cu_3(SE)_2(H_2O)_2Cl_3]Cl·6H_2O$ (**1**), $Cu_3(SE)_2(N_3)_4(DMF)_2$ (**2**), $Cu(SE)N_3·DMF$ (**3**) and $Cu(SE)N_3·Cu(SE)N_3$ (**4**) with tridentate Schiff-base ligands SE$^-$, derived from condensation of *N*,*N*-dimethylethylenediamine with salicylaldehyde, have been synthesised and characterised by IR spectroscopy, X-ray structural analyses and variable-temperature magnetic susceptibility measurements. Complex **1** has an alternating phenoxy- and chloro-bridged 1D chain structure. Complex **2** possesses trinuclear units in which the Cu^{II} ions are bridged by single end-on (μ-1,1) azido ligands. Uniformly spaced 1D chains with end-to-end (μ-1,3) azido bridges are found in **3** and **4**. As expected, complexes **1** and **2** exhibit antiferromagnetic and ferromagnetic exchange, respectively. Compounds **3** and **4** show unusual ferromagnetic coupling though the 1,3-azido pathways. Theoretical simulations have been carried out in order to evaluate the magnitude of the magnetic exchange and the magneto-structural correlation has been investigated.
(© Wiley-VCH Verlag GmbH & Co. KGaA, 69451 Weinheim, Germany, 2004)

Introduction

During the past decade, particular interest has been directed towards the investigation of copper(II) complexes with halogen bridging ligands as well as pseudohalogens, due to their correlative structures and ability to transmit magnetic interactions.[1−24] Among the ligands examined, the chloride anion has the capability of acting as either a bridging or a terminal ligand, occupying either axial or equatorial coordination positions. As a result, mono- or polynuclear complexes as well as 1D chain-like compounds have been obtained.[1−6] In addition, the azide ion is a versatile and popular pseudohalogen ligand due to its functionality as a bridging bi-, tri- and tetradentate ligand and its rich coordination behaviour, e.g. end-on (μ-1,1 and μ-1,1,1) or end-to-end (μ-1,3). These bridging ligands have yielded plenty of metal complexes with a wide variety of coordination geometries including tetrahedral or square-planar, trigonal-bipyramidal or square-pyramidal and octahedral, the geometry being dependent upon the coligands and the counterions.[8−24]

It has been reported that {*N*-[2-(dimethylamino)ethyl]-salicylaldiminato}copper(II) chloride, Cu(SE)Cl, can be synthesised in an anhydrous methyl/isopropyl alcohol medium.[7] A trinuclear complex $[Cu_3(\mu_3\text{-}OH)(SE)_3](ClO_4)_2(H_2O)_{0.5}$ containing a partially cubic Cu_3O_4 core was obtained from the reaction of $Cu(ClO_4)_2$ with SE$^-$ in a methanol/water solution.[6] We have found, in the absence of ClO_4^-, the reaction between $CuCl_2$ and SE$^-$ in a 1:1 molar ratio did not produce the expected 1:1 complex. Instead, a chain-like complex with the empirical formula $Cu_3(SE)_2(H_2O)_8Cl_4$ (**1**) was obtained which can be regarded as a mixture of $Cu(H_2O)_2Cl_2$ and Cu(SE)Cl (molar ratio = 1:2). It is worth noting that this complex exhibits an interesting and very rare structure, namely a 1D polymeric chain containing mixed bridges and hexa- and pentacoordinate copper atoms. The replacement of the bridging chloro ligands by azido ligands yields complexes with different structural types depending upon the solvents used (see Scheme 1). One example is the end-on azido-bridged trinuclear structure **2** $[Cu_3(SE)_2(N_3)_4(DMF)_2]$. $Cu(SE)N_3·DMF$ (**3**) possesses a uniformly spaced end-to-end azido-bridged copper(II) chain while $Cu(SE)N_3·Cu(SE)N_3$ (**4**) displays a chain structure similar to that of **3** with a cocrystallised mononuclear $Cu(SE)N_3$ unit. Herein, we report the syntheses, structural characterisation and magnetic properties of the four complexes.

Results and Discussion

Synthesis and General Characterisation

The trinuclear complex $[Cu_3(OH)(SE)_3](ClO_4)_2(H_2O)_{0.5}$ was always found to be the product from the reaction of $Cu(ClO_4)_2·6H_2O$ with SE$^-$ (molar ratio = 1:1).[6] We have observed that the employment of $CuCl_2·2H_2O$ instead of $Cu(ClO_4)_2·6H_2O$ results in the formation of the 1D chain complex $Cu_3(SE)_2(H_2O)_8Cl_4$ (Cu/SE$^-$, 3:2). The loss of the SE$^-$ ligand around a Cu^{II} ion may be due to the partial hydrolysis of the Schiff base while in anhydrous solvent environments 1:1 complexes were formed, as previously re-

---

[a] Department of Chemistry, Tsinghua University,
Beijing 100084, China
Fax: (internat.) + 86-10-62795477
E-mail: kouhz@mail.tsinghua.edu.cn

DOI: 10.1002/ejic.200400449

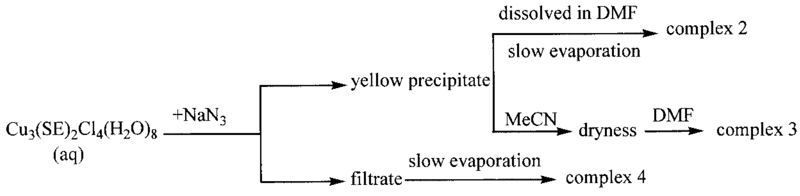

Scheme 1. Formation of Cu^{II} compounds

ported.[6,7] This observation indicates that the structures of Cu^{II}-SE$^-$ complexes vary with the synthetic conditions and counteranions used. Several complexes were obtained from the reaction of complex **1** with NaN$_3$.

The IR spectra of the complexes are similar and show peaks for the ν(C=N) bands at 1647 cm^{-1} in **1** and 1635 cm^{-1} in **2**, **3** and **4**, suggesting the presence of a Schiff base. The peaks at 1655 cm^{-1} in **2** and **3** can be reasonably attributed to the ν(C=O) of DMF. The appearance of a broad strong absorption at 3434 cm^{-1} in **1** indicates the presence of water molecules, consistent with the single-crystal X-ray diffraction results. Peaks at 2070 and 2031 cm^{-1} in the IR spectrum of **2** are due to the stretching of the μ-1,1 azide while the appearance of absorptions at 2074 and 2047 cm^{-1} in **3** and **4** is due to the asymmetric stretching of the μ-1,3 azide anions.

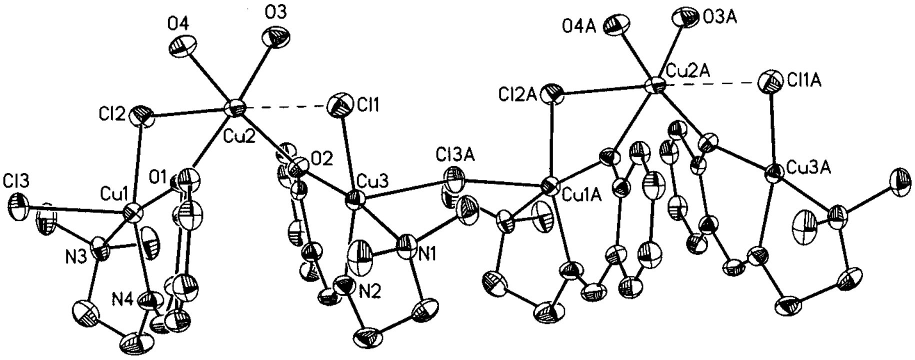

Figure 1. ORTEP representation of the cationic polymeric chain for **1** − 2.5H$_2$O with the atom labelling scheme showing 30% probability thermal ellipsoids; hydrogen atoms, solvent molecules and counterions have been omitted for clarity

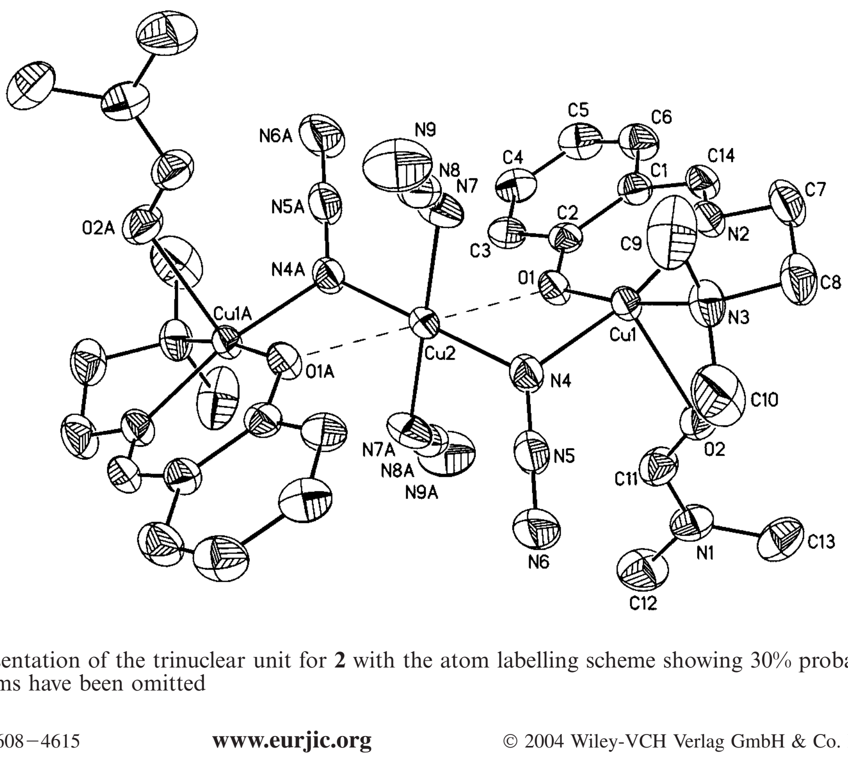

Figure 2. ORTEP representation of the trinuclear unit for **2** with the atom labelling scheme showing 30% probability thermal ellipsoids; for clarity hydrogen atoms have been omitted

Crystal Structures

The structures of **1−4** are displayed in Figures 1−4, respectively. Selected bond lengths and angles for complexes **1** − 2.5H_2O, **2**, **3** and **4** are listed in Tables 1−4, respectively.

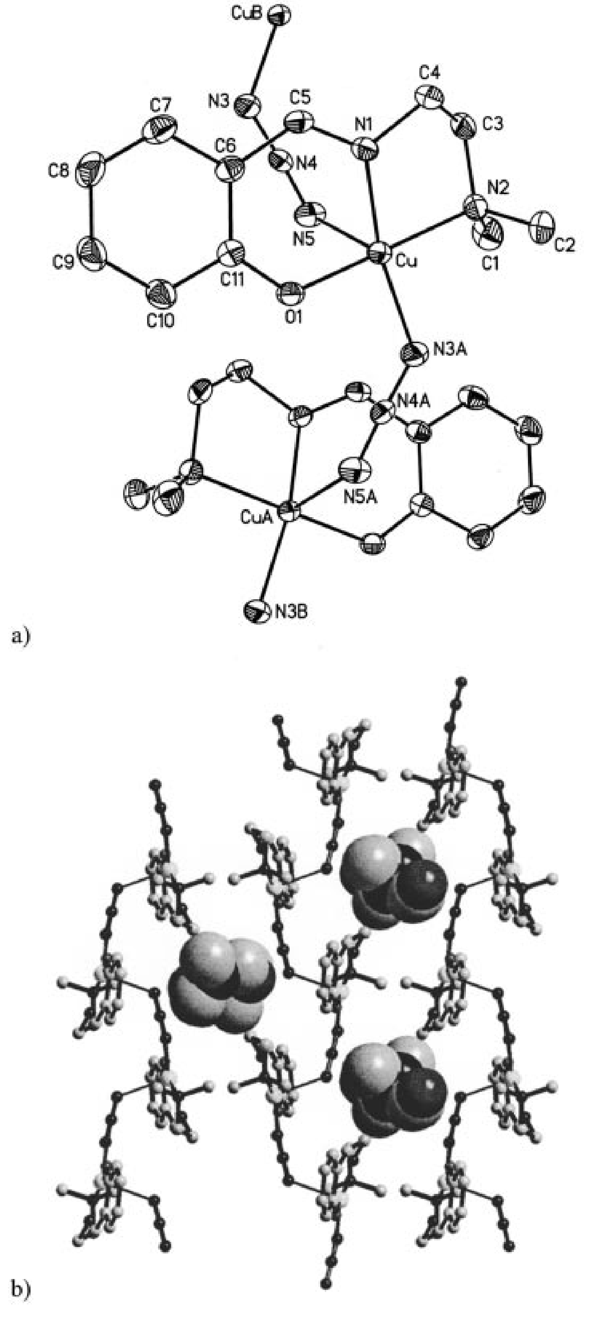

Figure 3. a) ORTEP representation of the 1D polymeric chain for **3** with the atom labelling scheme showing 30% probability thermal ellipsoids; for clarity hydrogen atoms and solvent DMF molecules have been omitted; b) view of the packing of the 1D chains in complex **3** (DMF was displayed in space-filling diagram)

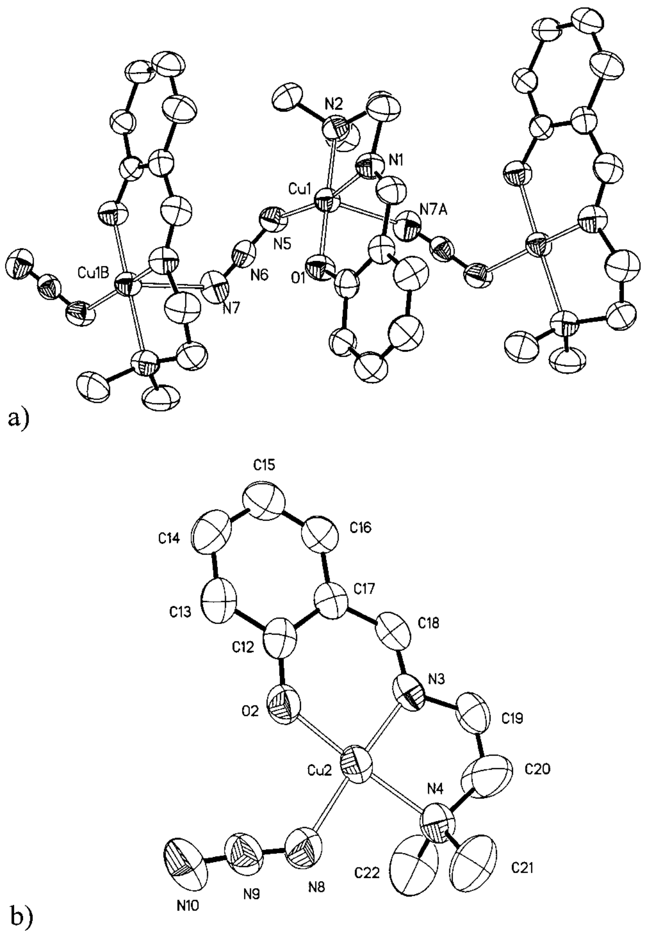

Figure 4. ORTEP representations of the structure of **4**: (a) the 1D chain, (b) the monomer with ellipsoids drawn at 30% probability level; for clarity hydrogen atoms have been omitted

The structure of **1** − 2.5H_2O consists of trinuclear cationic $[Cu_3(SE)_2(H_2O)_2Cl_3]_n^{n+}$ chains along the *a* axis formed by the chloro and phenolate oxygen bridges of SE^- (Figure 1), discrete Cl^- counteranions and solvated water molecules. Two of the copper atoms are pentacoordinate while the other is six-coordinate in the independent trinuclear fragment. Cu(1) and Cu(3) have slightly distorted square-pyramidal geometries as ascertained by the Reedijk factors τ of 0.113 and 0.132, respectively.[30] Cu(2) is in an elongated octahedral environment, being coordinated to two bridged chloro atoms [Cl(1) and Cl(2)] and four oxygen atoms, two of these being from water molecules [O(3) and O(4)] and two from the SE^- ligands [O(1) and O(2)]. For Cu(2), the Cu−Cl bonds [2.7176(15) and 2.7890(15) Å] are longer than Cu−O bonds [2.010(3), 1.984(4), 1.981(3) and 1.966(3) Å]. The elongated octahedron shares two equator-to-apex edges with the bases of two other square pyramids. The neighbouring pyramids share an apex occupied by a bridged chloro atom, yielding a 1D chain. Their basal planes, defined by N, N, O and Cl, are not coplanar and exhibit a dihedral angle of 21.1°, while the angles between these planes and the octahedral equatorial plane [O(1),O(2),O(3),O(4)] are 100° and 99.2°, respectively. Within the chain, the Cu(1)−Cu(2) distance is 3.257(7) Å, similar to the Cu(2)−Cu(3) distance of 3.223(7) Å, while the Cu(3)−Cu(1A) separation [5.161(14) Å] is very large.

Complex **2** contains a hexacoordinate and two pentacoordinate Cu^{II} ions which are bridged by the two end-on

Table 1. Selected bond lengths [Å] and angles [°] for **1** − 2.5H$_2$O

Cu(1)−N(5)	1.954(4)	Cu(1)−O(1)	1.994(3)
Cu(1)−N(3)	2.057(4)	Cu(1)−Cl(2)	2.2524(14)
Cu(1)−Cl(3)	2.5961(14)	Cu(2)−O(4)	1.966(3)
Cu(2)−O(2)	1.981(3)	Cu(2)−O(3)	1.984(4)
Cu(2)−O(1)	2.010(3)	Cu(2)−Cl(2)	2.7176(15)
Cu(2)−Cl(1)	2.7890(15)	Cu(3)−N(2)	1.958(4)
Cu(3)−O(2)	1.976(3)	Cu(3)−N(1)	2.071(4)
Cu(3)−Cl(1)	2.2577(15)	Cu(3)−Cl(3a)	2.5974(14)
N(5)−Cu(1)−O(1)	90.13(15)	N(5)−Cu(1)−N(3)	84.44(17)
O(1)−Cu(1)−N(3)	170.15(15)	N(5)−Cu(1)−Cl(2)	163.20(14)
O(1)−Cu(1)−Cl(2)	87.38(9)	N(3)−Cu(1)−Cl(2)	95.45(12)
N(5)−Cu(1)−Cl(3)	96.26(14)	O(1)−Cu(1)−Cl(3)	94.05(10)
N(3)−Cu(1)−Cl(3)	94.70(12)	Cl(2)−Cu(1)−Cl(3)	100.49(5)
O(4)−Cu(2)−O(2)	166.03(15)	O(4)−Cu(2)−O(3)	89.75(16)
O(2)−Cu(2)−O(3)	92.04(15)	O(4)−Cu(2)−O(1)	92.55(15)
O(2)−Cu(2)−O(1)	88.57(13)	O(3)−Cu(2)−O(1)	167.99(15)
O(4)−Cu(2)−Cl(2)	91.50(12)	O(2)−Cu(2)−Cl(2)	102.24(10)
O(3)−Cu(2)−Cl(2)	92.94(12)	O(1)−Cu(2)−Cl(2)	75.23(9)
N(2)−Cu(3)−O(2)	89.65(14)	N(2)−Cu(3)−N(1)	84.65(16)
O(2)−Cu(3)−N(1)	170.86(14)	N(2)−Cu(3)−Cl(1)	163.06(13)
O(2)−Cu(3)−Cl(1	88.47(10)	N(1)−Cu(3)−Cl(1)	94.90(12)
N(2)−Cu(3)−Cl(3a)	92.80(13)	O(2)−Cu(3)−Cl(3a)	92.79(10)
N(1)−Cu(3)−Cl(3a)	94.62(11)	Cl(1)−Cu(3)−Cl(3a)	104.10(5)
Cu(2)−Cl(1)−Cu(3)	78.60(13)	Cu(1)−Cl(2)−Cu(2)	81.38(4)
Cu(1)−O(1)−Cu(2)	108.99(13)	Cu(2)−O(2)−Cu(3)	109.05(14)

Symmetry operation: a: 1 − x, −y, 1 − z.

Table 2. Selected bond lengths [Å] and angles [°] for **2**

Cu(1)−O(1)	1.927(2)	Cu(1)−N(2)	1.941(3)
Cu(1)−N(4)	2.001(3)	Cu(1)−N(3)	2.050(3)
Cu(1)−O(2)	2.326(3)	Cu(2)−N(7a)	1.976(3)
Cu(2)−N(7)	1.976(3)	Cu(2)−N(4)	2.042(3)
Cu(2)−N(4a)	2.042(3)	Cu(2)−O(1)	2.468(3)
Cu(2)−O(1a)	2.468(3)		
O(1)−Cu(1)−N(2)	92.33(11)	O(1)−Cu(1)−N(4)	86.62(11)
N(2)−Cu(1)−N(4	169.19(13)	O(1)−Cu(1)−N(3)	172.15(12)
N(2)−Cu(1)−N(3)	84.33(13)	N(4)−Cu(1)−N(3	95.33(13)
O(1)−Cu(1)−O(2)	95.29(11)	N(2)−Cu(1)−O(2)	94.61(12)
N(4)−Cu(1)−O(2)	96.20(12)	N(3)−Cu(1)−O(2)	92.06(12)
N(7a)−Cu(2)−N(4)	91.60(15)	N(7)−Cu(2)−N(4)	88.40(15)
N(7)−Cu(2)−N(4a)	91.60(15)	Cu(1)−N(4)−Cu(2)	102.34(13)
N(6)−N(5)−N(4)	178.5(6)	Cu(2)−O(1)−Cu(1)	90.70(15)

Symmetry operation: a: −1 + x, y, z.

Table 3. Selected bond lengths [Å] and angles [°] for **3**

Cu−O(1)	1.9126(19)	Cu−N(1)	1.948(2)
Cu−N(3a)	1.974(3)	Cu−N(2)	2.067(2)
Cu−N(5)	2.474(2)		
O(1)−Cu−N(1)	92.76(9)	O(1)−Cu−N(3a)	92.42(10)
N(1)−Cu−N(3a)	167.08(10)	O(1)−Cu−N(2)	173.71(8)
N(1)−Cu−N(2)	84.05(10)	N(3a) −Cu−N(2)	89.63(11)
O(1)−Cu−N(5)	94.72(9)	N(1)−Cu−N(5)	88.81(9)
N(3a)−Cu−N(5)	102.55(10)	N(2)−Cu−N(5)	90.64(9)
N(5)−N(4)−N(3)	176.4(3)		

Symmetry operation: a: 0.5 + x, 1.5 − y, 2 − z.

Table 4. Selected bond lengths [Å] and angles [°] for **4**

Cu(1)−O(1)	1.905(4)	Cu(1)−N(1)	1.955(6)
Cu(1)−N(5)	1.972(7)	Cu(1)−N(2)	2.068(6)
Cu−N(7a)	2.604(6)	Cu(2)−O(2)	1.891(6)
Cu(2)−N(3)	1.926(6)	Cu(2)−N(8)	1.946(9)
Cu(2)−N(4)	2.072(7)		
O(1)−Cu(1)−N(1)	93.4(2)	O(1)−Cu(1)−N(5	92.4(2)
N(1)−Cu(1)−N(5)	164.8(3)	O(1)−Cu(1)−N(2)	177.2(2)
N(6a)−N(7a)−Cu(1)	124.4(3)	N(6)−N(5)−Cu(1)	121.0(5)
O(2)−Cu(2)−N(3)	93.2(3)	O(2)−Cu(2)−N(8)	92.0(4)
N(3)−Cu(2)−N(8)	173.2(5)	O(2)−Cu(2)−N(4)	176.3(3)
N(3)−Cu(2)−N(4)	84.3(3)	N(8)−Cu(2)−N(4)	90.7(4)
N(7)−N(6)−N(5)	177.1(8)	N(10)−N(9)−N(8)	177.0(12)

Symmetry operation: a: 0.5 − x, y, z − 0.5.

azido ligands (Figure 2). The central copper atom has an elongated octahedral coordination geometry with four azido nitrogen atoms (two terminal ligands, two end-on dicoordinated bridging ligands) in equatorial positions [Cu−N 1.976(3)−2.042(3) Å] and two phenoxy oxygen atoms from the SE$^-$ ligands in the axial positions (Cu−O 2.469 Å). Alternatively, the trinuclear structure of **2** is composed of two [Cu(SE)(DMF)]$^+$ cations connected by a [Cu(N$_3$)$_4$]$^{2-}$ anion through two azido ligands. Similar to complex **1**, the elongated octahedron shares two equator-to-vertex edges with the bases of two other square pyramids. With a τ factor of 0.048, the basal plane of the slightly distorted square pyramid is defined by N(2)−N(3)−N(4)-O(1) and the copper atom Cu(1) is 0.1570(5) Å above the basal plane towards the apical oxygen atom O(5) of the DMF molecule. The Cu−N−Cu angle is 102.34(13)°. It is evident that the basal planes of the square pyramids are perfectly coplanar, while the angle between these planes and the equatorial plane of the central copper ion is 70°. The intramolecular Cu(1)−Cu(2) distance is 3.150(5) Å.

The structure of **3** consists of end-to-end azido-bridged 1D infinite uniformly spaced chains with DMF molecules situated in the spaces between the chains (Figure 3). In the chain, each copper atom is coordinated by an SE$^-$ ligand and two azido ligands in a slightly distorted square-pyramidal arrangement (τ = 0.110). The basal plane is defined by N(1)−N(2)−N(3A)−O(1) and the copper atom is 0.1482(4) Å above the basal plane towards N(5) in the apical position. The angles between the copper ions and the azido ligands are 119.1(2)° [Cu−N(5)−N(4)] and 127.0(2)° [Cu−N(3A)−N(4A)] and the Cu−N$_3$−Cu torsion angle is 81.5°. The intrachain Cu−Cu distance is 5.530(4) Å, while the closest interchain Cu−Cu distance is 7.671(5) Å. Interstitial DMF molecules occupy interchain spaces and connect neighbouring 1D chains through van der Waals interactions and hydrogen bonds.

Complex **4** contains 1D chains similar to complex **3** with discrete Cu(SE)N$_3$ monomers beside the chains (Figure 4). In the chains, each copper atom is in a slightly distorted square-pyramidal arrangement with a τ factor of 0.200. The basal plane of the square pyramid is defined by N(1)−N(2)−N(5)−O(1) and Cu^{2+} is 0.1264(8) Å above the basal plane towards the bridging azido nitrogen atom N(7A) in the apical position. The bond angles between copper ions and azido ligands are 124.4(5)° [Cu(1)−N(7A)−N(6A)] and 121.0(5)° [Cu(1)−N(5A)−N(6A)] and the torsion angle (Cu−N_3−Cu) is 80.2°. The intrachain Cu−Cu distance is 5.392(2) Å. The copper atom in the monomer is in a square-planar arrangement and is tetracoordinated by SE^- and one terminal azido ligand. The chains and monomers form a complicated network by hydrogen bonds and van der Waals interactions.

Magnetic Properties

The $\chi_M T$ value at 300 K for **1** is 1.229 emu·K·mol^{-1} and this decreases slowly with decreasing temperature. The Weiss constant derived from the χ_m^{-1} vs. *T* plot is equal to −12.8 K with the Curie constant of 1.26 emu·K·mol^{-1} being close to the calculated value of 1.125 emu·K·mol^{-1} (g = 2.0) per Cu_3 unit. The overall behaviour of **1** corresponds to a weak antiferromagnetically coupled system. To evaluate the strength of the intermetallic exchange constants of **1**, we used an approximate approach similar to that previously used for 1D and quasi-2D complexes.[32] On the basis of the crystal data, for simplicity, the two coupling constants between Cu(1) and Cu(2) and between Cu(3) and Cu(2) which are bridged by the phenoxy and chloro bridges were assumed to be equal. The single axis-to-axis Cu−Cl−Cu coupling constants were considerably small compared with the coupling through the phenolate oxygen and the equator-to-vertex chloro bridges. Therefore, the 1D chain can be treated as being composed of weakly interacting trimers. The magnetic susceptibility data were fitted using the following expansion [Equation (1)] in which intertrimer and interchain exchanges were included in the parameter θ:

$$\chi_{\text{trimer}} = \frac{Ng^2\beta^2}{4kT}\left[\frac{1+\exp(-2J/kT)+10\exp(J/kT)}{1+\exp(-2J/kT)+2\exp(J/kT)}\right] \qquad (1)$$

$$\chi_M = \chi_{\text{trimer}}\frac{T}{T-\theta}$$

The results of the best fit, shown as the solid lines in Figure 5, are $J = -4.89\ \text{cm}^{-1}$, $g = 2.02$ and $\theta = -0.69$ K with the agreement factor $R = \Sigma[(\chi_M T)_{\text{obsd.}} - (\chi_M T)_{\text{calcd.}}]^2/\Sigma[(\chi_M T)^2_{\text{obsd.}}]$ of 6.7×10^{-4}.

Generally speaking, oxygen-bridging exchange interactions are much stronger than those involving halogens. On the basis of the structural data of **1**, the chloro-bridging conformation involves equator-to apex linkages [Cl(1) and Cl(2)] and axis-to-axis linkages [Cl(3)] while oxygen atoms occupy equator-to-equator positions. As a result, strong magnetic coupling with a large value ($|J| > 100\ \text{cm}^{-1}$) can be expected via the oxygen bridge. In our case, however, the observed superexchange interaction ($J = -4.89\ \text{cm}^{-1}$) is smaller than expected. We have ascribed the low superexchange to the small overlap of neighbouring Cu^{II} $d_{x^2-y^2}$ magnetic orbitals. If the $d_{x^2-y^2}$ orbitals interact in the same plane, strong coupling can be observed. In complex **1**, there are large dihedral angles of 100° and 99.2° between the oxygen-bridging copper orbital planes. The delocalisation is poor due to the small overlap and, consequently, the low superexchange can be understood.

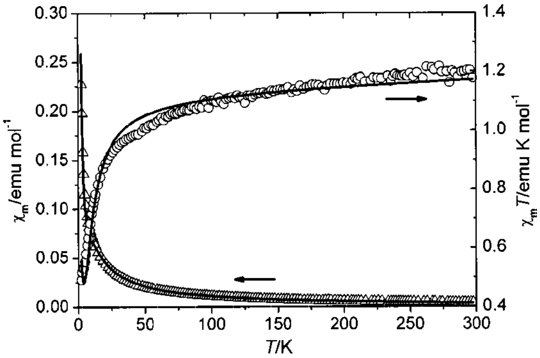

Figure 5. Plot of χ_M vs. *T* (open triangles) and $\chi_M T$ vs. *T* (open circles) for **1**; the solid lines represent the theoretical values based on the parameters described in the text

The temperature dependence of the magnetic susceptibility of complex **2** illustrated in Figure 6 suggests the presence of ferromagnetic coupling between the adjacent Cu^{II} ions. The Weiss constant derived from the χ_m^{-1} vs. *T* plot is equal to +12.1 K and the Curie constant of 1.31 emu·K·mol^{-1} is close to the calculated value of 1.125 emu·K·mol^{-1} (g = 2.0) per trimer. According to the crystal structure data, complex **2** has a symmetrical trinuclear entity which requires only one coupling constant. Similar to complex **1**, the magnetic susceptibility data can be successfully fitted using Equation (1) while intertrimeric exchange was included in the parameter θ. The best fit results, shown as the solid lines in Figure 6, are $J = +32.6\ \text{cm}^{-1}$, $g = 2.07$ and $\theta = -0.44$ K with $R = 1.6 \times 10^{-4}$.

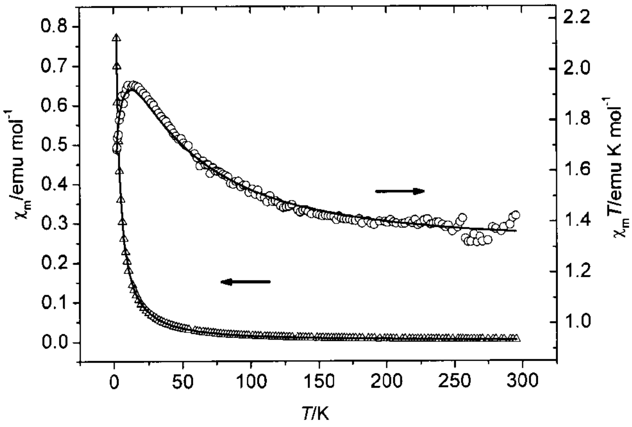

Figure 6. Plot of χ_M vs. *T* (open triangles) and $\chi_M T$ vs. *T* (open circles) for **2**; the solid lines represent the theoretical values based on the parameters described in the text.

Most of the $\mu_{1,1}$-azido bridged complexes are ferromagnetic as determined by the spin distribution in the spin triplet ground states according to the spin polarisation mechanism.[25,26] It has been widely cited that the superexchange interactions via the end-on azido bridges become antiferromagnetic at higher Cu−N−Cu angles.[8−13] From the density functional study by Ruiz et al., the critical angle is 104°.[8] Also, Thompson et al. suggested that the realm of ferromagnetic coupling ceases for angles greater than 108°.[9] However, an unprecedented low Cu−N−Cu angle of 89.1° was recently reported with an actual antiferromagnetic coupling.[13] This has been assumed to be due to minimal orbital overlap in a basal-axial fashion and a Cu−N distance (2.505 Å) longer than the cutoff distance (2.05 Å) for ferromagnetic interactions. In our case, the ferromagnetic coupling is in agreement with a Cu−N−Cu angle of 102.4° which is lower than the critical angle of 104° and the Cu−N distances [2.001(3) and 2.042(3) Å] are shorter than 2.05 Å. Generally speaking, the basal-to-basal coordination suggests a strong exchange coupling parameter and the actual value of +32.6 cm^{-1} for **2** can be understood in spite of the moderately large dihedral angle (70°) between the neighbouring Cu basal $d_{x^2-y^2}$ orbital planes. It should be mentioned that we have not considered the possible interaction through phenolate oxygen groups. Obviously, the superexchange interaction is negligible due to its basal-to-axial orientation and a long Cu−O distance [2.469(3) Å].

The gradual increase of $\chi_M T$ values with decreasing T for compounds **3** and **4** clearly indicates the existence of intrachain ferromagnetic interactions (Figures 7 and 8). The magnetic susceptibilities above 20.0 K obey the Curie−Weiss law with positive Weiss constants (θ) of +9.68 K for **3** and +6.3 K for **4**, suggesting the existence of ferromagnetic coupling between the adjacent Cu^{II} ions. The Curie constant (C) is equal to 0.355 emu·K·mol^{-1} for **3** which is close to the expected value of 0.375 emu K mol^{-1} and g = 2.0, while the Curie constant of 0.747 emu K mol^{-1} for **4** is in good agreement with the calculated value of 0.75 emu·K·mol^{-1} (g = 2.0). On the basis of the structural data for complex **3**, the magnetic susceptibility data were fitted using the 1D S = 1/2 expression based on the Hamiltonian $\hat{H} = -J\Sigma S_i S_{i+1}$. According to Kahn, no analytical expression has yet been proposed for the ferromagnetic Cu^{II} 1D system. However, a high-temperature series expansion, valid for both positive and negative J values, has been proposed.[27,28]

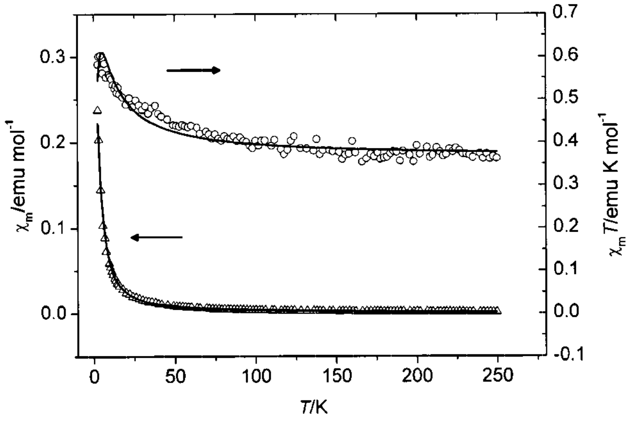

Figure 7. Plot of χ_M vs. T (open triangles) and $\chi_M T$ vs. T (open circles) for **3**; the solid lines represent the theoretical values based on the parameters described in the text

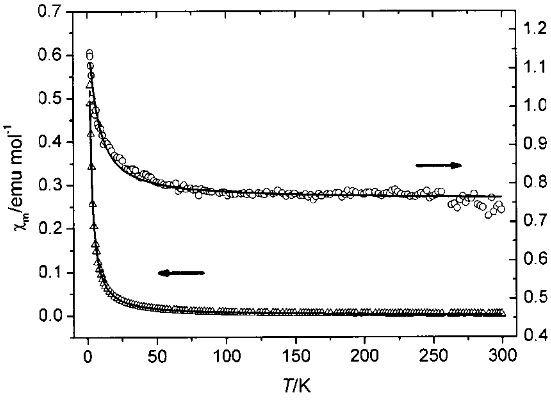

Figure 8. Plot of χ_M vs. T (open triangles) and $\chi_M T$ vs. T (open circles) for **4**; the solid lines represent the theoretical values based on the parameters described in the text

This expansion is:

$$\chi_{\text{chain}} = \frac{Ng^2\beta^2}{4kT}\left[\frac{A}{B}\right]^{2/3}$$

with $A = 1 + 5.7979916 \times x + 16.902653 \times x^2 + 29.376885 \times x^3 + 29.832959 \times x^4 + 14.036918 \times x^5$; $B = 1 + 2.7979916 \times x + 7.008678 \times x^2 + 8.6538644 \times x^3 + 4.5743114 \times x^4$ and $x = J/2kT$.

With the consideration of the interchain interactions:[29]

$$\chi_M = \frac{\chi_{chain}}{1-\chi_{chain}(2zJ'/Ng^2\beta^2)}$$

the best-fit results were obtained as J = +6.7 cm^{-1}, g = 2.0, zJ' = −1.3 cm^{-1} with $R = 1.5 \times 10^{-3}$.

Because complex **4** has a 1D chain similar to that in complex **3**, the magnetic susceptibilities of **4** were similarly simulated based on the chain model. The magnetic contribution of the discrete Cu(SE)N$_3$ monomer was added separately. All the non-intrachain interactions were included in the parameter zJ' using the molecular-field approximation.[29] This expansion is:

$$\chi_{chain} = \frac{Ng^2\beta^2}{4kT}\left[\frac{A}{B}\right]^{2/3}$$

$$\chi_{monomer} = \frac{Ng^2\beta^2}{4kT}$$

$$\chi_M = \frac{\chi_{chain} + \chi_{monomer}}{1-(\chi_{chain}+\chi_{monomer})(2zJ'/Ng^2\beta^2)}$$

The best fit results, as shown in Figure 8, are J = +4.64 cm^{-1}, g = 2.01 and zJ'= −0.30 cm^{-1} with $R = 2.6 \times 10^{-4}$.

For the end-to-end bridging mode of the azide, superexchange is generally antiferromagnetic in nature.[14,15,21−26] Recently, a few compounds have been reported to show a weak ferromagnetic interaction through the 1,3-bridging azido pathway.[16−20] It was found that in these unusual

Cu^{II} complexes, the bridging azido ligand involves an equatorial linkage to one Cu^{II} ion and an axial coordination to another Cu^{II} ion in the square-pyramidal or elongate octahedral geometry.[16] It is known that for the copper(II) ions, the unpaired electrons occupy the $d_{x^2-y^2}$ orbitals while the $d_z{}^2$ orbitals are filled with the paired electrons. Since the azido σ- and π-orbitals mainly overlap the full $d_z{}^2$ orbitals via the axial interaction, there is almost no coupling between them and thus magnetic coupling is expected to be weak. Furthermore, the 1,3-azido pathway superexchange coupling mainly depends on the Cu−N−N angle α and the Cu−N−N−N−Cu torsion angle θ. Large α and θ values may strongly reduce the antiferromagnetic component of superexchange. In our examples, the effects of the Cu−N−N angles were not drastic (below 104°), so the effect of torsion angles should be dominant. The antiferromagnetic component decreases with increasing θ and becomes zero when $\theta = 90°$ due to accidental orthogonality. The antiferromagnetic interactions then increase until reaching the maximum when $\theta = 180°$.[31] The Cu−N−N−N−Cu torsion angles of 81.5° for **3** and 80.2° for **4** (close to 90°) nullify the antiferromagnetic component and, as a result, net weak ferromagnetic interactions can be observed and explained on the basis of the above arguments.

Conclusion

The present report describes the syntheses, X-ray crystal structures and magneto-structural correlations of four novel phenoxy/chloro- and phenoxy/azido-bridged Cu^{II} complexes. The syntheses of the four compounds are intriguing and the final products are strongly dependent on the synthetic conditions. The $\chi_M T$ data for **1** and **2** were simulated using a trinuclear model, while the data for **3** and **4** were treated using a 1D infinite chain model for $S = 1/2$. The unusual ferromagnetic behaviour of the two $\mu_{1,3}$-N_3-bridged 1D complexes has been rationalised qualitatively on the basis of the axial-equatorial bridging mode as well as the $Cu-N_3-Cu$ torsion angles.

Experimental Section

General Remarks: Elemental analyses (C, H, N) were carried out with an Elementar Vario EL instrument. Infrared spectroscopy was performed with a Magna-IR 750 spectrophotometer in the 4000−400 cm^{-1} region. The TGA measurement of **1** was performed in the temperature range 20−300 °C under nitrogen with a Universal V2.6D TA instrument. Magnetic measurements were performed with a few single crystals (ca. 46 mg for **1**, 32.6 mg for **2**, 11.9 mg for **3** and 33.5 mg for **4**) using a MagLab 2000 magnetometer in a field of 10 kOe (**1**, **2** and **4**) or 20 kOe (**3**) from 2 to 300 K. The experimental susceptibilities were corrected for the diamagnetism of the constituent atoms (Pascal's Tables).

Caution! Although not encountered in our experiments, azido complexes of metal ions are potentially explosive. Only small amounts of the materials should be prepared and they should be handled with care.

Synthesis of 1: *N*,*N*-Dimethylethylenediamine (5.5 mL, 50 mmol) in methanol (10 mL) was mixed with salicylaldehyde (7.605 g, 50 mmol) in methanol (10 mL). $CuCl_2{\cdot}2H_2O$ (8.525 g, 50 mmol) in water (50 mL) was then added slowly and the mixture was heated to reflux for 0.5 h. The resultant dark green solution was reduced to 50 mL by rotary evaporation. Dark green needle-shaped single crystals suitable for X-ray analysis separated after several days. Yield: 4.44 g (31%). $C_{22}H_{46}Cl_4Cu_3N_4O_{10}$ (828.03): calcd. C 30.76, H 5.40, N, 6.52; found C 30.98, H 5.26, N 6.63. IR (KBr): $\tilde{\nu}$ = 3434 (O−H, H_2O), 1647 (C=N) cm^{-1}. The water content of **1** was confirmed by thermogravimetric analysis.

Syntheses of 2, 3 and 4: A slight excess of sodium azide (57 mg, 0.88 mmol), dissolved in a minimum amount of water, was added to an aqueous solution (10 mL) of **1** (170.2 mg, 0.2 mmol) with continuous stirring. This gave an immediate yellowish-brown precipitate which was collected by filtration and used for the following synthesis. Dark green platelet crystals of **4** were obtained by concentration of the filtrate at room temperature. Yield: 33.5 mg (30%). $C_{11}H_{15}CuN_5O$ (593.64): calcd. C 44.51, H 5.09, N 23.59; found C 44.26, H 5.07, N 24.20. IR (KBr): $\tilde{\nu}$ = 2074, 2048 (N_3), 1635(C=N) cm^{-1}. The yellow brown precipitate was directly dissolved in DMF (10 mL). Black block-shaped crystals suitable for X-ray analysis were formed by slow concentration at room temperature over several weeks. Pure **2** was obtained by manual separation under a microscope. Yield: 32.6 mg (19%). $C_{28}H_{44}Cu_3N_{18}O_4$ (887.43): calcd. C 37.90, H 5.00, N 28.41; found C 37.12, H 4.94, N 27.82. IR (KBr): $\tilde{\nu}$ = 2070, 2031 (N3), 1655 (C=O, DMF), 1636 (C=N) cm^{-1}. The yellow-brown precipitate was at first dissolved in MeCN (10 mL). After concentration to dryness, the resultant microcrystalline solid was collected and dissolved in DMF (10 mL). Slow concentration of the DMF solution gave bluish-green crystals of **3** suitable for X-ray analysis. Yield: 11.9 mg (8%). $C_{14}H_{22}CuN_6O_2$ (369.92): calcd. C 45.46, H 5.99, N 22.72; found C 44.16, H 5.73, N 23.16. IR (KBr): $\tilde{\nu}$ = 2074, 2047 (N_3), 1655 (C=O, DMF), 1634 (C=N) cm^{-1}.

X-ray Crystallographic Study: The data collections for **1** − $2.5H_2O$, **2**, **3** and **4** were made with a Bruker Smart CCD (293 K) and a Siemens Bruker P4 diffractometer, respectively. Intensity data were corrected for Lorentz and polarisation factors. Absorption corrections were applied using SADABS (Bruker 2000) (complexes **1** − $2.5H_2O$, **3** and **4**) and ψ-scan (complex **2**). The structures were solved by direct methods (SHELXS-97) and refined by full-matrix least squares (SHELXL-97) on F^2. Hydrogen atoms attached to the C and N atoms were added geometrically and refined using the riding model. In complex **1** − $2.5H_2O$, considerable disorder of the interstitial water molecules was observed and a split model was employed during the refinement. The crystal data are summarised in Table 5. CCDC-239759 to -239762 contain the supplementary crystallographic data for this paper. These data can be obtained free of charge at www.ccdc.cam.ac.uk/conts/retrieving.html [or from the Cambridge Crystallographic Data Centre, 12 Union Road, Cambridge CB2 1EZ, UK; Fax: + 44-1223-336-033; E-mail: deposit@ccdc.cam.ac.uk].

Acknowledgments

This work was supported by the National Natural Science Foundation of China (project nos. 20201008 and 50272034). We are grateful to Prof. Song Gao for the magnetic measurements.

Table 5. Crystal data for complexes **1** − 2.5H$_2$O, **2**, **3** and **4**

	1 − 2.5H$_2$O	**2**	**3**	**4**
Empirical formula	$C_{23}H_{43}Cl_4Cu_3N_4O_{7.5}$	$C_{28}H_{44}Cu_3N_{18}O_4$	$C_{14}H_{22}CuN_6O_2$	$C_{22}H_{30}Cu_2N_{10}O_2$
Formula mass	828.03	887.43	369.92	593.64
Space group	$P2_1/n$	$P2_1/c$	$P2_12_12_1$	$Pca2_1$
a [Å]	9.154(2)	10.7026(13)	9.3270(19)	21.783(3)
b [Å]	19.589(5)	17.4369(15)	12.049(2)	11.927(3)
c [Å]	18.371(5)	11.1640(15)	15.321(3)	10.207(2)
β [°]	94.677(6)	111.572(8)	90	90
V [Å^3]	3283.2(15)	1937.5(4)	1721.8(6)	2651.8(8)
Z	4	2	4	4
$\rho_{\mathrm{calcd.}}$ [g cm^{-3}]	1.675	1.521	1.427	1.487
μ(Mo-K_α) [mm^{-1}]	2.298	1.690	1.286	1.643
Data/restraint/parameters	5760/1/393	3412/0/241	6317/0/208	4193/1/325
GOF	1.064	1.006	1.158	0.992
$R1$ [$I > 2\sigma(I)$]	0.0458	0.0388	0.0552	0.0468
$wR2$ (all data)	0.1183	0.1135	0.0981	0.1582

---

[1] S. Haddad, R. D. Willett, *Inorg. Chem.* **2001**, *40*, 2457−2460.

[2] M. Y. Wei, R. D. Willett, *Inorg. Chem.* **1996**, *35*, 6381−6385.

[3] R. Bhattacharya, A. Ghosh, M. S. Ray, L. Righi, G. Bocelli, S. Chaudhuri, R. D. Willett, J. M. Clemente-Juan, E. Coronado, C. J. Goméz-Garicia, *Eur. J. Inorg. Chem.* **2002**, 4253−4259.

[4] M. Hernández-Molina, J. González-Platas, C. Ruiz-Pérez, F. Lloret, M. Julve, *Inorg. Chim. Acta* **1999**, *284*, 258−265.

[5] A. M. Schuitema, A. F. Stassen, W. L. Driessen, J. Reedijk, *Inorg. Chim. Acta* **2002**, *337*, 48−52.

[6] H.-D. Bian, J.-Y. Xu, W. Gu, S.-P. Yan, P. Cheng, D.-Z. Liao, Z.-H. Jiang, *Polyhedron* **2003**, *22*, 2927−2932.

[7] E. W. Hatfield, F. L. Bunger, *Inorg. Chem.* **1968**, *8*, 1194−1195.

[8] E. Ruiz, J. Cano, S. Alvarez, P. Alemany, *J. Am. Chem. Soc.* **1998**, *120*, 11122−11129.

[9] S. S. Tandon, L. K. Thompson, M. E. Manuel, I. N. Bridson, *Inorg. Chem.* **1994**, *33*, 5555−5570.

[10] L. K. Thompson, S. S. Tandon, M. E. Manuel, *Inorg. Chem.* **1995**, *34*, 2356−2366.

[11] P. S. Mukherjee, T. K. Maji, G. Mostafa, T. Mallah, N. R. Chaudhuri, *Inorg. Chem.* **2000**, *39*, 5147−5150.

[12] E.-Q. Gao, S.-Q. Bai, C.-F. Wang, Y.-F. Yue, C.-H. Yan, *Inorg. Chem.* **2003**, *42*, 8456−8464.

[13] S. Koner, S. Saha, T. Mallah, K.-I. Okamoto, *Inorg. Chem.* **2004**, *43*, 840−842.

[14] C. G. Pierpont, D. N. Hendrickson, D. M. Duggan, F. Wagner, E. K. Barefield, *Inorg. Chem.* **1975**, *14*, 604−610.

[15] A. Escuer, R. Vicente, J. Ribas, M. S. El Fallah, X. Solans, *Inorg. Chem.* **1993**, *32*, 1033−1035.

[16] C. S. Hong, Y. Do, *Angew. Chem. Int. Ed.* **1999**, *38*, 193−195.

[17] P. S. Mukherjee, S. Dalai, E. Zangrando, F. Lloret, N. R. Chaudhuri, *Chem. Commun.* **2001**, 1444−1445.

[18] [18a] P. S. Mukherjee, T. K. Maji, A. Escuer, R. Vicente, J. Ribas, G. Rosair, F. A. Mautner, N. R. Chaudhuri, *Eur. J. Inorg. Chem.* **2002**, 943−949. [18b] S. Dalai, P. S. Mukherjee, M. G. B. Drew, T.-H. Lu, N. R. Chaudhuri, *Inorg. Chim. Acta* **2002**, *335*, 85−90. [18c] S. Dalai, P. S. Mukherjee, T. Mallah, M. G. B. Drew, N. R. Chaudhuri, *Inorg. Chem. Commun.* **2002**, *5*, 472−474. [18d] T. K. Maji, P. S. Mukherjee, G. Mostafa, T. Mallah, J. Cano-Boquera, N. R. Chaudhuri, *Chem. Commun.* **2001**, 1012−1013. [18e] P. S. Mukherjee, S. Dalai, G. Mostafa, T.-H. Lu, E. Rentschler, N. R. Chaudhuri, *New J. Chem.* **2001**, *25*, 1203−1207.

[19] L.-C. Li, D.-Z. Liao, Z.-H. Jiang, S.-P. Yan, *Inorg. Chem.* **2002**, *41*, 1019−1021.

[20] B. Woodard, R. D. Willett, S. Haddad, B. Twamley, C. J. Gomez-Garcia, E. Coronado, *Inorg. Chem.* **2004**, *43*, 1822−1824.

[21] C. R. Choudhuri, S. K. Dey, R. Karmakar, C.-D. Wu, C.-Z. Lu, M. S. El Fallah, S. Mitra, *New J. Chem.* **2003**, *27*, 1360−1366.

[22] S. K. Dey, N. Mondal, M. S. El Fallh, R. Vicente, A. Escuer, X. Solans, M. Font-Bardfa, T. Matsushita, V. Gramlich, S. Mitra, *Inorg. Chem.*, in press.

[23] S. S. Tandon, L. K. Thompson, D. O. Miller, *J. Chem. Soc., Chem. Commun.* **1995**, 1907−1908.

[24] L. K. Thompson, S. S. Tandon, F. Lloret, J. Cano, M. Julve, *Inorg. Chem.* **1997**, *36*, 3301−3306.

[25] J. Comarmond, P. Plumere, J.-M. Lehn, Y. Agnus, R. Louis, R. Weiss, O. Kahn, I. Morgenstern-Badarau, *J. Am. Chem. Soc.* **1982**, *104*, 6330−6340.

[26] M.-F. Charlot, O. Kahn, M. Chaillet, C. Larried, *J. Am. Chem. Soc.* **1986**, *108*, 2574−2581.

[27] O. Kahn, *Molecular Magnetism*, VCH, Weinheim, **1993**, chapter 6.

[28] G. A. Baker, G. S. Rushbrooke, H. E. Gilbert, *Phys. Rev.* **1964**, *135*, A1272.

[29] C. J. O'Conner, *Prog. Inorg. Chem.* **1982**, *29*, 203.

[30] A. W. Addison, T. N. Rao, J. Reedijk, J. V. Rijin, G. C. Verschoor, *J. Chem. Soc., Dalton Trans.* **1984**, 1349.

[31] A. Escuer, R. Vicente, J. Ribas, M. S. El Fallah, X. Solans, M. Font-Bardia, *Inorg. Chem.* **1993**, *32*, 3727−3732.

[32] [32a] S. G. Kang, K. Ryu, S.-K. Jung, J. Kim, *Inorg. Chim. Acta* **1999**, *293*, 140. [32b] B. Chiari, A. Cinti, O. Piovesana, P. F. Zanazzi, *Inorg. Chem.* **1995**, *34*, 2652−2657.

Received May 282004
Early View Article